

Effect of Ca on the Properties of Gd-Doped Ceria for IT-SOFC

S. Ramesh¹, G. Upender¹, K. C. James Raju¹, G. Padmaja², S. Mohan Reddy², C. V. Reddy²

¹School of Physics, University of Hyderabad, Hyderabad, India

²Department of Physics, Osmania University, Hyderabad, India

Email: ramesh.oul@gmail.com

Received March 20, 2013; revised April 23, 2013; accepted May 18, 2013

Copyright © 2013 S. Ramesh *et al.* This is an open access article distributed under the Creative Commons Attribution License, which permits unrestricted use, distribution, and reproduction in any medium, provided the original work is properly cited.

ABSTRACT

Ceria based electrolyte materials are very useful in intermediate-temperature solid oxide fuel cell (IT-SOFC). The compositions $\text{Ce}_{0.85}\text{Gd}_{0.15-x}\text{Ca}_x\text{O}_{2-\delta}$ ($x = 0.0 - 0.075$) were prepared through sol-gel method. Their structure was studied by X-ray diffraction. Dense ceramic $\text{Ce}_{0.85}\text{Gd}_{0.15-x}\text{Ca}_x\text{O}_{2-\delta}$ samples were prepared by sintering the pellets at 1300°C. The lattice parameter was calculated by Rietveld refinement of XRD patterns. Four probe A.C. impedance spectroscopy was used to study the total ionic conductivity of doped and co-doped ceria ceramics in the temperature range 200°C - 700°C. The $\text{Ce}_{0.85}\text{Gd}_{0.125}\text{Ca}_{0.025}\text{O}_{2-\delta}$ composition showed maximum ionic conductivity with less activation energy.

Keywords: Ceramic; Sol-gel Process; Activation Energy; Electrical Conductivity; Solid Electrolyte

1. Introduction

Solid oxide fuel cells are the energy converters; they convert chemical energy of fuel to electrical energy. Recently Solid oxide fuel cells (SOFC) have been attracting more attention due to high efficiency and clean energy. Yttria-stabilized zirconia (YSZ) is a standard electrolyte for solid oxide fuel cell applications. High operating temperatures (1000°C) are required to increase the ionic conductivity of YSZ. However, at such high operating temperatures there are some problems like thermal mismatch between cell components, chemical instability, selection of materials etc. [1,2].

Doped ceria electrolytes showed higher ionic conductivity at relatively low temperatures 350°C - 700°C. In comparison to that of yttria stabilized zirconia (YSZ) and ceria doped with heterovalent cations, such as rare earth and alkaline earth ions have been extensively studied as most promising electrolyte materials for intermediate temperature solid oxide fuel cells (IT-SOFC) [1].

Among the various dopants studied, gadolinium doped ceria (GDC) has been reported to have the highest ionic conductivity [3].

As reported in the literature [4-13], the co-doping could enhance the ionic conductivity. Dopant ion, dopant concentration, oxygen vacancy concentration and defect association energy and local defect structure are the factors, which can influence the total ionic conductivity in

doped ceria [3,14].

In the present work, we have selected divalent (Ca^{2+}) and trivalent (Gd^{3+}) as co-dopants because their effective ionic radii are closer to critical radius (r_c). In order to develop intermediate temperature electrolyte material for solid oxide fuel cell, Gd^{3+} and Ca^{2+} co-doped ceria based materials $\text{Ce}_{0.85}\text{Gd}_{0.15-x}\text{Ca}_x\text{O}_{2-\delta}$ ($x = 0.0, 0.025, 0.05$ and 0.075) are prepared and characterized. The main aim is to study the structure and electrical conductivity of the Ca co-doped ceria in comparison with gadolinium-doped ceria ($\text{Ce}_{0.85}\text{Gd}_{0.15}\text{O}_{2-\delta}$).

2. Experimental

Sol-gel method [4,5] was used to synthesize the samples with the general formula $\text{Ce}_{0.85}\text{Gd}_{0.15-x}\text{Ca}_x\text{O}_{2-\delta}$ ($x = 0.0, 0.025, 0.05$ and 0.075). High purity cerium nitrate ($\text{Ce}(\text{NO}_3)_3 \cdot 6\text{H}_2\text{O}$), gadolinium nitrate ($\text{Gd}(\text{NO}_3)_3 \cdot 6\text{H}_2\text{O}$) and calcium nitrate ($\text{Ca}(\text{NO}_3)_2 \cdot 4\text{H}_2\text{O}$) were used as starting materials. Experimental results can be obtained elsewhere [4,5]. The resultant ash was ground in agate mortar to get a fine homogeneous powder. Then the powders were pressed uni-axially with the help of hydraulic press under a continuous pressure of 5 Mpa for 5 min into a circular pellet using a stainless steel die of dimensions 10 mm in diameter and 2 mm in thickness and then pellets were sintered in air at 1300°C for 8 h with a programmed heating rate of 5°C min^{-1} . The densities of sintered sam-

ples were measured in water using the Archimedes method. The sintered samples have more than 96% of the theoretical density.

X-ray diffraction patterns of the samples were obtained by Bruker D8 advanced X-ray diffractometer (XRD) using Cu K α radiation (1.54056 Å) operated at 40 kV, 30 mA at room temperature, in the Bragg's angle range of $20^\circ \leq 2\theta \leq 80^\circ$ with a scan rate of 2° min^{-1} . The lattice parameter was calculated rietveld refinement of XRD data. FE-SEM was used to take surface images.

Electrical impedance (Z) and phase angle (θ) were measured using Agilent impedance analyzer (4294 A) in the frequency range 42 Hz - 5 MHz on dense sintered pellet. Zsimpwin software was used to analyze the impedance data and to calculate the total ionic conductivity of the samples. The electrical conductivity measurements were taken at various temperatures in the temperature range $200^\circ\text{C} - 700^\circ\text{C}$ in air. Silver paste was brushed to each side of the samples, which was subsequently dried (at 600°C for 15 min) producing solid silver electrode on both sides of the pellet.

3. Results and Discussion

3.1. Structure Analysis

To confirm the phase formation, dissolution of dopants in CeO_2 lattice, XRD patterns were measured for calcium co-doped ceria ceramics as shown in **Figure 1(a)**. Calcium co-doped ceria samples show that the samples contain only a cubic fluorite structure with the space group $\text{Fm}\bar{3}\text{m}$ (JCPDS powder diffraction File No. 34-0394).

Figure 1(b) shows the rietveld refinement of $\text{Ce}_{0.85}\text{Gd}_{0.125}\text{Ca}_{0.025}\text{O}_{2-\delta}$ sample. Structure analysis and Lattice parameter was calculated using Rietveld refinement software.

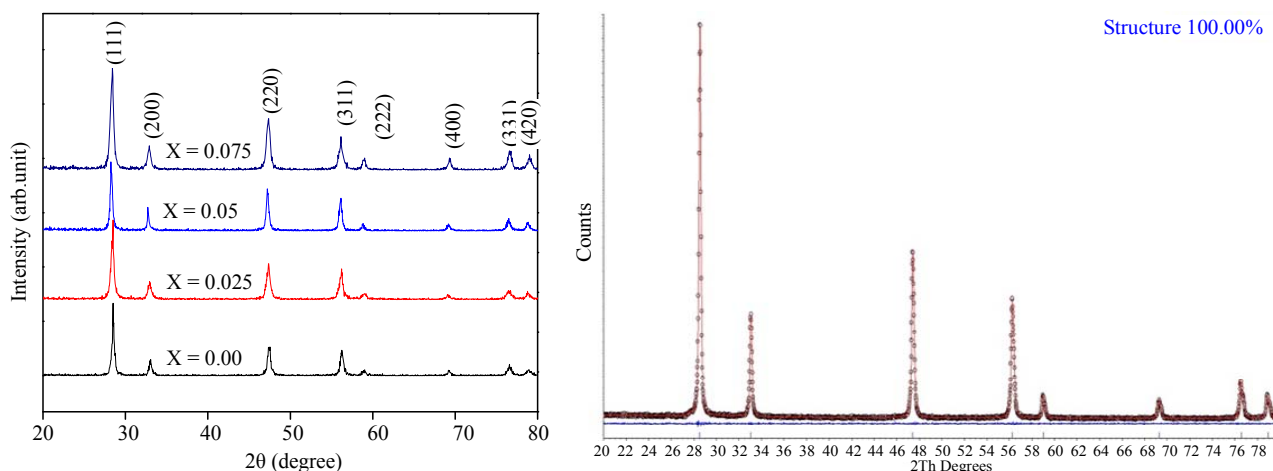


Figure 1. (a) XRD patterns of $\text{Ce}_{0.85}\text{Gd}_{0.15-x}\text{Ca}_x\text{O}_{2-\delta}$ system. **(b)** Rietveld refinement of $\text{Ce}_{0.85}\text{Gd}_{0.125}\text{Ca}_{0.025}\text{O}_{2-\delta}$. (Black color: Experimental, Red color: Fitted, Blue color: Difference).

Figure 2 shows the lattice parameter as a function of dopant concentration. Lattice parameter increases linearly with an increase in dopant concentration (Ca). This indicates the validation of Vegard's rule.

The lattice parameter increased with an increase in the Ca amount. This is due to difference in ionic radii of Ce^{4+} (0.96 \AA), Ca^{2+} (1.12 \AA) and Gd^{3+} (1.053 \AA) [15]. The introduction of Gd^{3+} and Ca^{2+} into Ce^{4+} can cause a small shift in the ceria peaks. This shift is indicative of change in the lattice parameter. As the Ca content increases, the lattice parameter increases for $\text{Ce}_{0.85}\text{Gd}_{0.15-x}\text{Ca}_x\text{O}_{2-\delta}$ ($x = 0.0 - 0.075$) samples. This indicates that Ca dissolved into the Ce sites in $\text{Ce}_{0.85}\text{Gd}_{0.15-x}\text{Ca}_x\text{O}_{2-\delta}$ system.

Figure 3 shows the cross sectional view of broken pellet of SEM picture of $\text{Ce}_{0.85}\text{Gd}_{0.125}\text{Ca}_{0.025}\text{O}_{2-\delta}$ sample. It can be seen that few closed pores are presented.

3.2. Impedance Spectroscopy

Figure 4 shows the Nyquist plots of $\text{Ce}_{0.85}\text{Gd}_{0.125}\text{Ca}_{0.025}\text{O}_{2-\delta}$ ceramic sample at 300°C . It is noticed that incomplete depressed arc, complete semi-circle and a part of arc are clearly seen. High frequency depressed arc corresponds to grain resistance (R_b), intermediate frequency semi-circle corresponds to grain boundary resistance (R_{gb}) and low frequency incomplete arc corresponds to electrode resistance (R_e). Grain and grain boundary resistance arcs are well-resolved at 300°C . In this case the equivalent circuit (**Figure 4**) is used to fit the impedance data and to calculate grain (R_b) and grain boundary resistance (R_{gb}). The use of simple capacitor is not sufficient to model the electrical response of the materials due to depression of arcs in some cases. For this purpose a constant phase element (CPE) is used to fit the results [16]. Electrode resistance is not considered for the total conductivity calculations in the present paper.

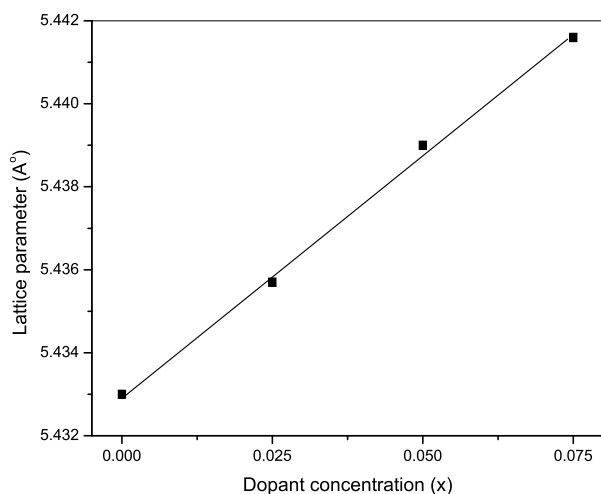


Figure 2. Lattice parameter of $\text{Ce}_{0.85}\text{Gd}_{0.15-x}\text{Ca}_x\text{O}_{2-\delta}$ system.

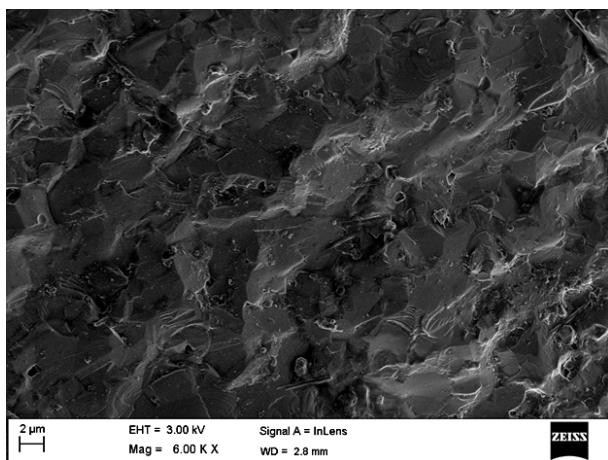


Figure 3. SEM image of $\text{Ce}_{0.85}\text{Gd}_{0.125}\text{Ca}_{0.025}\text{O}_{2-\delta}$ sample.

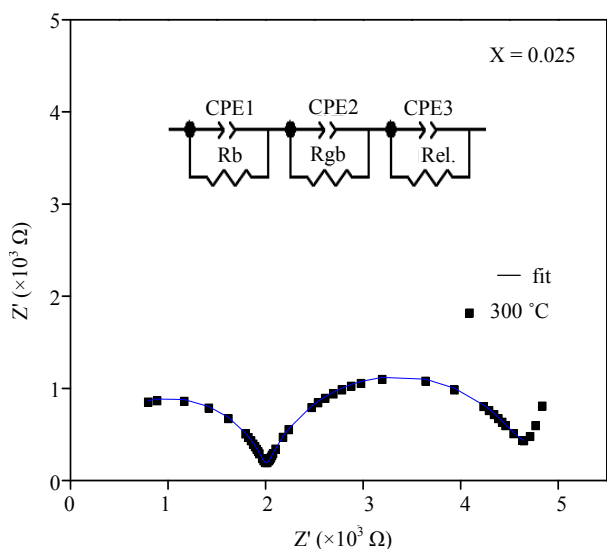


Figure 4. Impedance spectrum of $\text{Ce}_{0.85}\text{Gd}_{0.125}\text{Ca}_{0.025}\text{O}_{2-\delta}$ sample.

3.3. Electrical Conductivity

The sample total resistance, R_t can be obtained from impedance spectroscopy at different temperatures as,

$$R_t = R_g + R_{gb}$$

The total electrical conductivity σ was then calculated using equation,

$$\sigma_t = \frac{1}{R_t} * \frac{l}{A}$$

where l is the thickness, A is the cross sectional area of the sample.

The main contribution of the conductivity of ceria-based compounds in air is the ionic conductivity and the contribution of electronic conductivity is negligible [1, 2,16]. In this paper the conductivity measured in air can be treated as oxide ion conductivity.

The activation energy for conduction is obtained by plotting the ionic conductivity data in the Arrhenius relation for thermally activated conduction using equation,

$$\sigma T = \sigma_o \exp\left(-\frac{E_a}{kT}\right)$$

where E_a is the activation energy for conduction, T is the absolute temperature, k is the Boltmann's constant and σ_o is a pre-exponential factor. The equation may be linearised by plotting a logarithmic relationship between $\log(\sigma T)$ and $1000/T$

Figure 5 shows the Arrhenius plots for total ionic conductivity of $\text{Ce}_{0.85}\text{Gd}_{0.15-x}\text{Ca}_x\text{O}_{2-\delta}$ ($x = 0.0 - 0.075$) ceramics. The doping of trivalent oxides into ceria creates oxygen vacancies, which are responsible for the ionic conduction in these oxides [1,2]. In cerium oxide (CeO_2) oxide vacancies may be introduced by ceria reduction or by doping with oxides of metals with lower valences. These equations are written in Kröger-Vink notation [1,3].



The addition of gadolinium and calcium into cerium oxide (CeO_2) would create oxygen vacancies at low dopant concentration. From Figure 5 it can be seen that the conductivities of gadolinium and calcium co-doped ceria ($x = 0.025$ and 0.05) are higher than the single-doped ceria

The activation energies of $\text{Ce}_{0.85}\text{Gd}_{0.15-x}\text{Ca}_x\text{O}_{2-\delta}$ ($x = 0.0 - 0.075$) ceramics are shown in Table 1. The change in activation energy is attributed to an order and disorder transition of the oxygen sublattice [1]. The activation energy is minimum (Table 1) for the composition

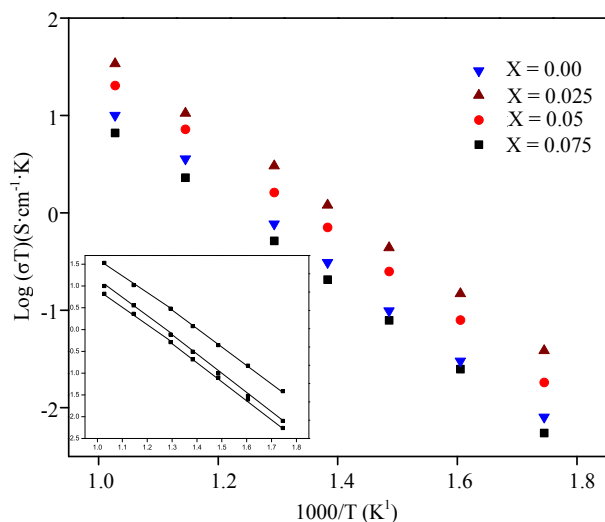


Figure 5. Arrhenius plots of $\text{Ce}_{0.85}\text{Gd}_{0.15-x}\text{Ca}_x\text{O}_{2-\delta}$ system (Inset fig. shows linear fitting).

Table 1. Activation energy of $\text{Ce}_{0.85}\text{Gd}_{0.15-x}\text{Ca}_x\text{O}_{2-\delta}$ system.

Composition	Activation energy (eV)	
	Total ionic Conductivity	
	200°C - 500°C ± 0.01°C	500°C - 700°C ± 0.01°C
$x = 0.00$	0.88	0.83
$x = 0.025$	0.83	0.78
$x = 0.05$	0.85	0.82
$x = 0.075$	0.89	0.84

$\text{Ce}_{0.85}\text{Gd}_{0.125}\text{Ca}_{0.025}\text{O}_{2-\delta}$. This decrease in activation energy is due to the presence of attractive interactions between dopant cations and oxygen vacancies [1,3]. Further, an increase in the Ca dopant content for $\text{Ce}_{0.85}\text{Gd}_{0.15-x}\text{Ca}_x\text{O}_{2-\delta}$ ($x = 0.0 - 0.075$) system, co-dopant prevents oxygen-ordering leading to an increase in activation energy and decrease in ionic conductivity in ceria solid solutions.

Moreover, activation energy (E_a) is the sum of the association enthalpy (ΔH_a) and migration enthalpy (ΔH_m) for conduction. At lower temperatures, activation energy depends on these two contributions. At higher temperatures, activation energy is equal to the migration enthalpy, because oxygen vacancies are free to diffuse [1,3]. Activation energy values for total ionic conduction of Ca co-doped ceria materials are calculated using least-squares linear regression (Figure 4).

From the Figure 5 and Table 1, it is noticed that the composition $\text{Ce}_{0.85}\text{Gd}_{0.125}\text{Ca}_{0.025}\text{O}_{2-\delta}$ showed highest total ionic conductivity and minimum activation energy. The total ionic conductivity of the composition $\text{Ce}_{0.85}\text{Gd}_{0.125}\text{Ca}_{0.025}\text{O}_{2-\delta}$ is $0.0127 \text{ S}\cdot\text{cm}^{-1}$ at 500°C . Sha

et al. reported that the total conductivity for $\text{Ce}_{0.8}\text{Gd}_{0.1}\text{Y}_{0.1}\text{O}_{1.9}$ was $0.0129 \text{ S}\cdot\text{cm}^{-1}$ at 600°C [8]. Yanyi et al. [9] reported that the electrical conductivity for $\text{Ce}_{0.8}\text{Sm}_{0.1}\text{Nd}_{0.1}\text{O}_{1.9}$ was 0.0122 S/cm at 500°C . By contrast with the literature, the present test sample is a possible electrolyte for intermediate temperature solid oxide fuel cell.

4. Conclusion

Co-doped ceria samples successfully synthesized through sol-gel process. All compositions showed cubic structure. Over 96% of relative density was obtained. Co-dopants improved the electrical conductivity of Gd-doped ceria.

5. Acknowledgements

S. Ramesh thanks the University Grants Commission (UGC), New Delhi, India for financial assistance under the Dr. D. S. Kothari postdoctoral fellowship (DSKPDF) scheme.

REFERENCES

- [1] H. Inaba and H. Tagawa, *Solid State Ionics*, Vol. 83, 1996, pp. 1-16. doi:10.1016/0167-2738(95)00229-4
- [2] J. A. Kilner, *Solid State Ionics*, Vol. 129, 2000, pp. 13-23. doi:10.1016/S0167-2738(99)00313-6
- [3] B. C. H. Steele, *Solid State Ionics*, Vol. 129, 2000, pp. 95-110. doi:10.1016/S0167-2738(99)00319-7
- [4] S. Ramesh, V. P. Kumar, P. Kistaiah and C. Vishnuvardhan Reddy, *Solid State Ionics*, Vol. 181, 2010, pp. 86-91. doi:10.1016/j.ssi.2009.11.014
- [5] S. Ramesh and C. Vishnuvardhan Reddy, *Acta Physica Polonica A*, Vol. 115, 2009, pp. 909-913.
- [6] H. D. Wiemhofer, *Solid State Ionics*, Vol. 117, 1999, pp. 229-243. doi:10.1016/S0167-2738(98)00408-1
- [7] K. Kim, B. H. Kim and D. Lee, *Journal of Power Sources*, Vol. 90, 2000, pp. 139-143. doi:10.1016/S0378-7753(00)00389-X
- [8] Y. Liu, B. Li B, X. Wei and W. J. Pan, *Journal of the American Ceramic Society*, Vol. 91, 2008, pp. 3926-3930. doi:10.1111/j.1551-2916.2008.02748.x
- [9] X. Sha, Z. Lu, X. Huang, J. Miao, Z. Liu, X. Xin, Y. Zhang and W. Su, *Journal of Alloys and Compounds*, Vol. 433, 2007, pp. 274-278. doi:10.1016/j.jallcom.2006.06.062
- [10] F. Y. Wang, B. Z. Wan and S. Cheng, *Journal of Solid State Electrochemistry Communications*, Vol. 9, 2005, pp. 168-173.
- [11] F. Y. Wang, S. Chen, Q. Wang, S. Yu and S. Cheng, *Catalysis Today*, Vol. 97, 2004, pp. 189-194. doi:10.1016/j.cattod.2004.04.059
- [12] N. Cioatera, V. Parvulescu, A. Rolle and R. N. Vannier, *Solid State Ionics*, Vol. 180, 2009, pp. 681-687. doi:10.1016/j.ssi.2009.02.025

- [13] Y. F. Zheng, H. T. Gu, H. Chen, L. Gao, X. F. Zhu and L. C. Guo, *Materials Research Bulletin*, Vol. 44, 2009, pp. 775-779. [doi:10.1016/j.materresbull.2008.09.021](https://doi.org/10.1016/j.materresbull.2008.09.021)
- [14] H. Yoshida, T. Inagaki, K. Miura, M. Inaba and Z. Ogumi, *Solid State Ionics*, Vol. 160, 2003, pp. 109-116. [doi:10.1016/S0167-2738\(03\)00153-X](https://doi.org/10.1016/S0167-2738(03)00153-X)
- [15] R. D. Shannon, *Acta Crystallographica Section A*, Vol. 32, 1976, pp. 751-767. [doi:10.1107/S0567739476001551](https://doi.org/10.1107/S0567739476001551)
- [16] W. Lai and S. M. Haile, *Journal of the American Ceramic Society*, Vol. 89, 2005, pp. 2979-2997. [doi:10.1111/j.1551-2916.2005.00740.x](https://doi.org/10.1111/j.1551-2916.2005.00740.x)